Kinetics of Two Pathways for 4,6-Dimethyldibenzothiophene Hydrodesulfurization over NiMo, CoMo Sulfide, and Nickel Phosphide Catalysts

ARTICLE *in* ENERGY & FUELS · FEBRUARY 2005

Impact Factor: 2.79 · DOI: 10.1021/ef049804g

3 AUTHORS, INCLUDING:

Xiaoliang Ma
Kuwait Institute for Scientific Research
112 PUBLICATIONS **4,576** CITATIONS
SEE PROFILE

Chunshan Song
Pennsylvania State University
462 PUBLICATIONS **11,775** CITATIONS
SEE PROFILE

Kinetics of Two Pathways for 4,6-Dimethyldibenzothiophene Hydrodesulfurization over NiMo, CoMo Sulfide, and Nickel Phosphide Catalysts

Jae Hyung Kim, Xiaoliang Ma, and Chunshan Song*

Clean Fuels and Catalysis Program, The Energy Institute, and Department of Energy & Geo-Environmental Engineering, The Pennsylvania State University, 209 Academic Projects Building, University Park, Pennsylvania 16802

Yong-Kul Lee and S. Ted Oyama

Environmental Catalysis and Materials Laboratory, Department of Chemical Engineering, Virginia Polytechnic Institute and State University, Blacksburg, Virginia 24061

Received August 4, 2004. Revised Manuscript Received November 3, 2004

The kinetics for the initial stage of the hydrodesulfurization (HDS) of 4,6-dimethyldibenzothiophene (4,6-DMDBT) and dibenzothiophene (DBT) were comparatively examined over NiMo and CoMo sulfide catalysts and newly developed nickel phosphide catalysts. The HDS can proceed through an indirect hydrogenation (HYD) pathway and a direct desulfurization (DDS, or hydrogenolysis) pathway. The rate constants for the HYD and DDS pathways (k_1 and k_2, respectively) were estimated using a method that involved extrapolation to zero conversion for the initial selectivity ratio of primary products. The overall rate constants ($k_1 + k_2$) for 4,6-DMDBT on a catalyst weight basis (in units of 10^{-5} s^{-1} $g{\cdot}cat^{-1}$) at 573 K under a pressure of 20.4 atm increased in the order of CoMo sulfide (34.1) < Ni_2P/USY (51.5) < Ni_2P/SiO_2 (66.4) < NiMo sulfide (83.2); however, the values based on active sites (in units of s^{-1} active $site^{-1}$) ranked in a different order (CoMo sulfide (4.0) < NiMo sulfide (8.8) < Ni_2P/USY (15.2) < Ni_2P/SiO_2 (23.7)). The rate constants for the HYD pathway of 4,6-DMDBT HDS at 573 K based on active sites were strongly dependent on the type of catalyst used; however, those for the DDS pathway were less sensitive to the type of catalyst, as can be observed from the corresponding values (k_1; k_2) for CoMo sulfide (2.2; 1.8), NiMo sulfide (6.7; 2.1), Ni_2P/USY (12.7; 2.5), and Ni_2P/SiO_2 (21.6; 2.1). The NiMo sulfide catalyst, which favored the HYD pathway, was more active than the CoMo sulfide catalyst for 4,6-DMDBT. The nickel phosphide catalysts showed higher activity in 4,6-DMDBT HDS than the sulfide catalysts, based on rate constants normalized to active sites; they operated through the HYD pathway. A comparison with DBT HDS at 573 K under a hydrogen (H_2) pressure of 20.4 atm showed that the presence of the methyl groups at the 4- and 6-positions dramatically inhibited the DDS pathway, because of steric hindrance around the S atom, and thus made the HYD pathway more important. Higher H_2 pressure further enhanced the HYD pathway, whereas increased temperature increased the contribution of the DDS pathway for 4,6-DMDBT HDS.

1. Introduction

Deep hydrodesulfurization (HDS) of diesel fuel is an important research area, because of increasingly stringent environmental regulations for fuel sulfur content.[1−9] The sulfur level in diesel fuel must be reduced from the present maximum of 500 ppmw (parts per million by weight) of sulfur to 15 ppmw by 2006 and further lower sulfur regulations are expected in the future; therefore, numerous studies on deep HDS of diesel fuel are being conducted.[1,2,6−12] Approaches investigated include (a) improving the catalytic activity of the molybdenum

* Author to whom correspondence should be addressed. Telephone: 814-863-4466. Fax: 814-865-3248. E-mail address: csong@psu.edu.

(1) Girgis, M. J.; Gates, B. C. *Ind. Eng. Chem. Res.* **1991**, *30*, 2021. Song, C. S.; Ma, X. L. *Appl. Catal. B: Environ.* **2003**, *41* 207.

(2) Song, C. S. *Catal. Today* **2003**, *86*, 211. Breysse, M.; Djega-Mariadassou, G.; Pessayre, S.; Geantet, C.; Vrinat, M.; Perot, G.; Lemaire, M. *Catal. Today* **2003**, *84*, 129.

(3) Topsøe, H.; Clausen, B.; Massoth, F. E. *Hydrotreating Catalysis*; Springer−Verlag: Berlin, Heidelberg, 1996; Chapter 1.

(4) Babich, I. V.; Moulijn, J. A. *Fuel* **2003**, *82*, 607.

(5) Prins, R. *Adv. Catal.* **2001**, *46*, 399. Ho, T. C. *Catal. Rev.—Sci. Eng.* **1988**, *30*, 117.

(6) Ma, X.; Sakanishi, K.; Mochida, I. *Ind. Eng. Chem. Res.* **1994**, *33*, 218. Ho, T. C. *Appl. Catal. A: Gen.* **2003**, *244*, 115. Turaga, U. T.; Song, C. S. *Catal. Today* **2003**, *86*, 129. Turaga, U. T.; Song, C. S. *Catal. Today* **2003**, *86*, 265.

(7) Whitehurst, D. D.; Isoda, T.; Mochida, I. *Adv. Catal.* **1998**, *42*, 345.

(8) Startsev, A. N. *Catal. Rev.—Sci. Eng.* **1995**, *37*, 353.

(9) Kwak, C.; Lee, J. J.; Bae, J. S.; Moon, S. H. *Appl. Catal., B: Environ.* **2001**, *35*, 59.

(10) Kabe, T.; Aoyama, Y.; Wang, D.; Ishihara, A.; Qian, W.; Hosoya, M.; Zhang, Q. *Appl. Catal., A: Gen.* **2001**, *209*, 237.

(11) Oyama, S. T.; Wang, X.; Lee, Y.-K.; Bando, K.; Requejo, F. G. *J. Catal.* **2002**, *210*, 207.

(12) Stinner, C.; Prins, R. Weber, Th. *J. Catal.* **2001**, *202*, 187.

10.1021/ef049804g CCC: $30.25
Published on Web 02/04/2005

Table 1. Composition and Properties of CoMo and NiMo Sulfide and Nickel Phosphide Catalysts

Catalyst	Content (wt %) MoO_3	Content (wt %) Co or Ni	Support	Surface Area (m^2/g)	Pore Volume (cm^3/g)	Density (cm^3/g)	Active Sites (μmol/g)
Cr344	13.5 (9.0[a])	2.9 CoO	Al_2O_3	183.3	0.48	0.74	85.9[b]
Cr424	13.0 (8.7[a])	3.0 NiO	Al_2O_3	163.2	0.40	0.81	95.0[b]
Ni_2P/USY		5.9 Ni	USY-Zeolite[c]	530.0	0.43		34.0[d]
Ni_2P/SiO_2		5.9 Ni	SiO_2 (EH-5)	170.0	0.80		28.0[d]

[a] Content of metal (in wt %). [b] Measured by oxygen chemisorption. [c] SiO_2/Al_2O_3 ratio is 80. [d] Measured by CO chemisorption.

sulfide catalysts used currently in the refining industry,[7,10] (b) developing new catalysts,[11−13] (c) tailoring reaction and process conditions,[14] and (d) designing new reactor configurations.[14] In all these approaches, information on the HDS kinetics of the refractory sulfur compounds in diesel fuel will be useful for making improvements.

Recent investigations of the HDS reactivity of various sulfur compounds have demonstrated that sulfur compounds remaining in diesel fuels at sulfur levels of <500 ppmw are dibenzothiophenes (DBTs) with alkyl substituents at the 4- and/or 6-position.[6] Of these, 4,6-dimethyldibenzothiophene (4,6-DMDBT) has been reported as one of the most refractory sulfur compounds in diesel fuel,[7,15,16] and, consequently, has been used as a model sulfur compound for deep HDS of diesel fuel.[7,17−19]

The HDS of DBTs generally proceeds through two pathways: a hydrogenation (HYD) pathway involving aromatic ring hydrogenation, followed by C−S bond cleavage, and a hydrogenolysis pathway via direct C−S bond cleavage without aromatic ring hydrogenation, which is also called the direct desulfurization (DDS) pathway.[20,21] The HDS of DBT occurs predominantly via the DDS pathway; however, the HYD pathway becomes more important for the HDS of 4,6-DMDBT. For deep HDS, new catalysts with higher hydrogenation activity are required, and, to evaluate new catalysts and design new deep HDS processes, kinetic data for each reaction pathway of 4,6-DMDBT HDS are important. However, such kinetic data are still very limited in the literature.[7,17,22−26]

The present study is focused on examining the kinetics of two different pathways over the sulfide catalysts and recently developed nickel phosphide catalysts. To get the reliable individual rate constants for DBTs HDS, we have compared three different methods in our previous study[27] and found that the initial selectivity method is better, because it does not require any assumptions about the individual steps in the reaction network. Therefore, the initial selectivity method is used in this study to estimate the individual rate constants. The HDS mechanism of 4,6-DMDBT is discussed on the basis of the determined kinetic constants and results of computational studies of the reacting molecules.

2. Experimental Section

The reagents—4,6-DMDBT, DBT, and decahydronaphthalene (Decalin, used as solvent)—were purchased from Aldrich Chemical Company and were used without further purification. For the HDS of 4,6-DMDBT, its concentration was 1.23 wt % (0.81 mol %) in Decalin. For the HDS of DBT, its concentration was 1.07 wt % (0.81 mol %) in Decalin.

HDS was conducted in a batch reactor with a volume of 25 mL. The reactor was loaded with 0.1 g of catalyst and 4.0 g of Decalin fuel containing 4,6-DMDBT or DBT, and the assembly was then purged five times with nitrogen and hydrogen, respectively, before being pressurized with hydrogen to the desired initial pressure. The reactor was placed in a fluidized sand bath, which was preheated to the desired temperature and agitated at a rate of 200 strokes/min, at which no effect of the external diffusion on the HDS conversion was observed under the conditions used in this study. The temperature inside the reactor was monitored by a thermocouple. Following the reaction, the reactor was removed from the sand bath and immediately quenched in a cold-water bath. A gas chromatography−mass spectroscopy (GC−MS) system (Shimadzu model GC17A/QP-500) was used for identification of the products, whereas a gas chromatograph (SRI 8610C) equipped with a flame ionization detector (FID) was used for quantitative analysis of the products.

Two commercial catalysts—$CoMo/Al_2O_3$ (Cr344) and $NiMo/Al_2O_3$ (Cr424), obtained from the Criterion Catalyst Company—were used for the HDS of 4,6-DMDBT and DBT. The chemical composition and textural properties of these catalysts are shown in Table 1. The catalysts were crushed to a particle size of <1 mm and presulfided at 623 K for 4 h in a flow of 5 vol % H_2S-H_2 at a flow rate of 200 mL/min and were subsequently stored in Decalin to minimize oxidation.

Nickel phosphide (Ni_2P) catalysts, supported on ultrastable Y zeolite USY (CBV780 in its hydrogen form, from Zeolyst; SiO_2/Al_2O_3 molar ratio = 80) or SiO_2 (Cab-O-Sil EH-5, from Cabot), were also examined for the HDS of 4,6-DMDBT. The catalysts were prepared by impregnating an aqueous nickel phosphate solution onto the predried USY and SiO_2 (EH-5) supports, followed by drying, calcination at 773 K for 5 h, and temperature-programmed reduction (at a heating rate of 1 K/min to 938 K, followed by holding at that temperature for 2 h).[11] For the kinetic study, the phosphide catalysts were pretreated in a H_2 flow at 693 K for 4 h and then stored in Decalin before use.

(13) Oyama, S. T. *J. Catal.* **2003**, *216*, 343.
(14) Sie, S. T. *Fuel Process. Technol.* **1999**, *61*, 149.
(15) Ma, X.; Sakanishi, K.; Mochida, I. *Ind. Eng. Chem. Res.* **1996**, *35*, 2487.
(16) Gates, B. C.; Topsoe, H. *Polyhedron* **1997**, *16*, 3213.
(17) Farag, H.; Whitehurst, D. D.; Sakanishi, K.; Mochida, I. *Catal. Today* **1999**, *50*, 49.
(18) Bataille, F.; Lemberton, J.-L.; Michaud, P.; Perot, G.; Vrinat, M.; Lemaire, M.; Schulz, E.; Breysse, M.; Kasztelan, S. *J. Catal.* **2000**, *191*, 409.
(19) Da Costa, P.; Potvin, C.; Manoli, J.-M.; Lemberton, J.-L.; Perot, G.; Djega-Mariadassou, G. *J. Mol. Catal. A* **2002**, *184*, 323.
(20) Broderick, D. H.; Gates, B. C. *AIChE J.* **1981**, *27*, 663.
(21) Ma, X.; Sakanishi, K.; Isoda, T.; Mochida, I. In *Hydrotreating Technology for Pollution Control*; Occelli, M. L., Chianelli, R., Eds.; Marcel Dekker: New York, 1996; p 183. Sakanishi, K.; Nagamatsu, T.; Mochida, I.; Whitehurst, D. *J. Mol. Catal. A* **2000**, *155*, 101.
(22) Whitehurst, D. D.; Farag, H.; Nagamatsu, T.; Sakanishi, K.; Mochida, I. *Catal. Today* **1998**, *45*, 299.
(23) Farag, H.; Mochida, I.; Sakanishi, K. *Appl. Catal., A: Gen.* **2000**, *194−195*, 147.
(24) Steiner, P.; Blekkan, E. A. *Fuel Process. Technol.* **2002**, *79*, 1.
(25) Singhal, G. H.; Espino, R. L.; Sobel, J. E.; Huff, G. A., Jr. *J. Catal.* **1981**, *67*, 457.
(26) Vrinat, M. L. *Appl. Catal.* **1983**, *6*, 137.
(27) Kim, J. H.; Ma, X.; Song, C.; Oyama, T.; Lee, Y.-K. *Prepr. Pap.—Am. Chem. Soc., Div. Fuel Chem.* **2003**, *48* (1), 40.

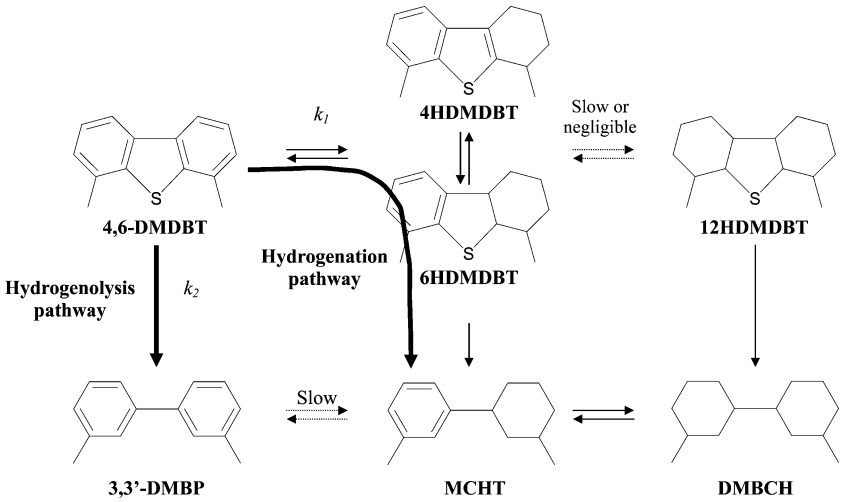

Figure 1. Scheme of 4,6-dimethyldibenzothiophene (4,6-DMDBT) hydrodesulfurization (HDS) via a ring hydrogenation network (denoted by the rate constant k_1) and a direct C−S bond hydrogenolysis network (denoted by the rate constant k_2).

Irreversible O_2 and CO uptake measurements were performed to estimate the number of active sites on the sulfide and phosphide catalysts, respectively. After pretreatment of the catalysts, calibrated pulses of O_2 at dry ice/acetone temperature (for sulfide catalysts) or CO at room temperature (for phosphide catalysts) in a helium carrier flowing at 26.7 μmol/s (40 cm^3 NTP min^{-1}) were injected through a sampling valve and the mass 32 (O_2) and 28 (CO) signals were monitored with a mass spectrometer.

All quantum-chemical calculations were performed using a semiempirical (PM3) method in the CAChe MOPAC program. The MOPAC-PM3 method determines both the optimum geometry and electronic properties of molecules by solving the Schrödinger equation, using PM3 semiempirical Hamiltonians that have been developed by Stewart.[28]

3. Results

3.1. HDS Studies. The network of reactions of 4,6-DMDBT is shown in Figure 1. The hydrogenation (HYD) and direct desulfurization (DDS, or hydrogenolysis) routes are indicated by arrows.

To obtain reliable kinetic data, experiments were conducted under conditions that would give 4,6-DMDBT conversions of <20%. The main products of 4,6-DMDBT HDS were tetrahydrodimethyldibenzothiophene (4HDMDBT), 3,3′-dimethylbiphenyl (DMBP), and methylcyclohexyltoluene (MCHT). 3,3′-Dimethylbicyclohexane (DMBCH) was also detected over NiMo sulfide when the reaction time was >7 min. However, it was detected over CoMo sulfide only under certain reaction conditions, such as 573 K and a H_2 pressure of 40.8 atm. Hexahydrodimethyldibenzothiophene (6HDMDBT) was also detected over the NiMo sulfide under all reaction conditions; however, it was observed in the HDS over the CoMo sulfide only under high hydrogen pressure. Dodecahydrodimethyldibenzothiophene (12HDMDBT) was not observed at all in the HDS products over these catalysts under the conditions that were utilized.

Table 2 summarizes the product distribution in the HDS of 4,6-DMDBT and DBT at different temperatures and H_2 pressures over the NiMo and CoMo sulfide catalysts. The conversions of DBT over these two catalysts were very similar: ∼20% for reaction at 573 K under an H_2 pressure of 20.4 atm for 17 min. However, the conversion of 4,6-DMDBT was considerably higher with the NiMo than with the CoMo sulfide (15.6% vs 8.5%, respectively) for reaction under the same conditions for 22 min at 573 K. As shown in Table 2, the conversions of 4,6-DMDBT were higher for all the runs with NiMo sulfide than the corresponding runs with CoMo sulfide. This is consistent with what we expected, because NiMo sulfide is more active for hydrogenation.

In the HDS of DBT, biphenyl (BP) is a main product and is formed over CoMo sulfide with ∼85% selectivity and over NiMo sulfide with ∼64% selectivity. The selectivities for the partially hydrogenated product (cyclohexylbenzene, CHB) and the fully hydrogenated product (bicyclohexane, BCH) are considerably lower. The sum of the selectivities for the hydrogenated products amounts to 14.2% for the CoMo sulfide and 35.6% for the NiMo sulfide. In the HDS of 4,6-DMDBT, however, the hydrogenated products (HDMDBTs and MCHT) are the main products. The selectivity of these products is much higher, compared to the selectivity of DMBP, which is the product of DDS. The selectivity for hydrogenated products is ∼85% over the NiMo sulfide and ∼70% over the CoMo sulfide under all reaction conditions. It is likely that nickel favors the HYD pathway because it is a good hydrogenation catalyst.[29]

In this work, the reaction temperature was varied between 548 K and 598 K at the constant initial H_2 pressure of 20.4 atm. The conversion of 4,6-DMDBT increased as the reaction temperature increased. Among the hydrogenated products, the selectivity for HDMDBTs over the NiMo sulfide decreased from 55.7% at 548 K to 31.7% at 598 K. However, the DDS product (DMBP) was not changed significantly: ∼15% under these conditions. Over the CoMo sulfide catalyst, the effect of temperature was very similar. The effect of H_2 pressure on the catalytic performance was also studied at 573 K. The results show that the conversion increased as the H_2 pressure increased. The DDS product over the NiMo sulfide decreased from 15.2% at 13.6 atm to 8.6%

(28) Stewart, J. J. P. *J. Comput. Chem.* **1989**, *10*, 209. Stewart, J. J. P. *J. Comput. Chem.* **1989**, *10*, 221.

(29) Marinas, J. M.; Campelo, J. M.; Luna, D. *Stud. Surf. Sci. Catal.* **1986**, *27* 411.

Table 2. Conversion and Product Distributions for HDS of 4,6-DMDBT and DBT over Sulfide Catalysts under Different Conditions

	20.4 atm, 548 K	20.4 atm, 573 K	20.4 atm, 598 K	13.6 atm, 573 K	40.8 atm, 573 K
			4,6-DMDBT[a]		
NiMo Sulfide					
conversion (%)	11.1	15.6	24.5	15.1	21.9
selectivity (%)					
DMBCH	4.9	7.0	7.4	4.4	11.5
MCHT	25.2	36.9	44.2	30.7	46.5
DMBP	14.2	12.4	16.7	15.2	8.6
HDMDBT[c]	55.7	43.7	31.7	49.7	33.4
CoMo Sulfide					
conversion (%)	6.6	8.5	11.4	8.4	9.6
selectivity (%)					
DMBCH	0.0	0.0	0.0	0.0	3.6
MCHT	38.2	45.1	49.9	45.2	56.2
DMBP	26.0	30.1	31.0	28.4	19.6
HDMDBT[c]	35.8	24.8	19.1	26.4	20.6
			DBT[b]		
NiMo Sulfide					
conversion (%)		22.9			
selectivity (%)					
BCH		1.9			
CHB		33.7			
BP		64.4			
CoMo Sulfide					
conversion (%)		20.7			
selectivity (%)					
BCH		0.4			
CHB		13.8			
BP		85.8			

[a] Product distribution of 4,6-DMDBT HDS after 22 min. [b] Product distribution of DBT HDS after 17 min. [c] Sum of tetrahydrodimethyldibenzothiophene (4HDMDBT) and hexahydrodimethyldibenzothiophene (6HDMDBT).

at 40.8 atm at 573 K. A similar trend was also observed over the CoMo sulfide catalyst.

3.2. Overall Rate Constants of 4,6-Dimethyldibenzothiophene Hydrodesulfurization. As a first approximation, the HDS of individual sulfur compounds follows pseudo-first-order kinetics,[15,30] whereas mixtures of gas oils and heavier oils may follow pseudo-second-order kinetics[14] or a linear combination of pseudo-first-order kinetics.[1] Integrating the first-order rate expression for 4,6-DMDBT HDS results in the following expression:

$$\ln\left(\frac{C_{\mathrm{DMDBT}}}{C_{\mathrm{DMDBT}_0}}\right) = -(k_1 + k_2)t \qquad (1)$$

where k_1 is the rate constant for the hydrogenation (HYD) pathway, k_2 is the rate constant for the hydrogenolysis (DDS) pathway, and $k_1 + k_2$ represents the overall HDS rate constant of 4,6-DMDBT. This overall HDS rate constant can be obtained from the experimental data. Figure 2 and Table 3 show the kinetic results and the overall rate constants of 4,6-DMDBT and DBT HDS over the NiMo and CoMo sulfide catalysts. The experimental data follow pseudo-first-order kinetics.

The overall rate constant for 4,6-DMDBT HDS at 573 K and 20.4 atm with the NiMo sulfide was 83.2×10^{-5} s^{-1} g·cat^{-1}, whereas that with the CoMo sulfide was 34.1×10^{-5} s^{-1} g·cat^{-1}. As described previously, the NiMo sulfide was more active than the CoMo sulfide and this is probably because the NiMo sulfide catalyst has higher hydrogenation activity.

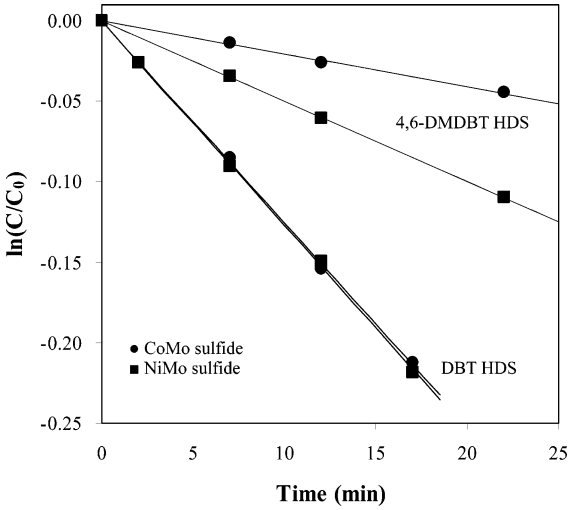

Figure 2. Pseudo-first-order kinetics of 4,6-DMDBT and DBT HDS over the NiMo and CoMo sulfide catalysts. Temperature = 573 K, H_2 pressure = 20.4 atm.

On the other hand, the two catalysts were more active but showed much less difference in overall rates for the HDS of DBT. The overall DBT HDS rate constant over the sulfided NiMo was 212.3×10^{-5} s^{-1} g·cat^{-1}, and that over the sulfided CoMo was 209.6×10^{-5} s^{-1} g·cat^{-1}. Further examination of the product distribution reveals that there are major differences in the contributions of the different reaction pathways: more hydrogenated products were formed over the NiMo sulfide than over the CoMo sulfide. This also highlights the need to obtain

(30) Houalla, M.; Broderick, D. H.; Sapre, A. V.; Nag, N. K.; De Beer, V. H.; Gates, B. C.; Kwart, H. *J. Catal.* **1980**, *61*, 523.

Table 3. Overall Rate Constants for HDS of 4,6-DMDBT and DBT over the Sulfided NiMo and CoMo Catalysts

	Overall Rate Constant, $k_1 + k_2$ ($\times 10^{-5}$ s^{-1} g·cat^{-1})[a]				
Catalyst	20.4 atm, 548 K	20.4 atm, 573 K	20.4 atm, 598 K	13.6 atm, 573 K	40.8 atm, 573 K
		4,6-DMDBT			
NiMo sulfide	60.0	83.2	159.3	55.2	133.5
CoMo sulfide	13.5	34.1	66.5		43.8
		DBT			
NiMo sulfide		212.3			
CoMo sulfide		209.6			

[a] Overall hydrodesulfurization of 4,6-dimethyldibenzothiophene or dibenzothiophene.

the individual rate constants for each reaction pathway, because the overall rate constants do not indicate which reaction pathway is more important with a given catalyst system.

3.3. Individual Rate Constant of 4,6-Dimethyldibenzothiophene Hydrodesulfurization. Although the overall HDS rate constant was obtained directly from the experimental data using eq 1, the individual rate constants for each reaction pathway are not easy to measure. Some researchers tried to estimate these values using equations that were derived with some assumptions.[17,19,21] However, these methods are not easy to use for calculating the rate constants directly from the experimental results. Since $k_1 + k_2$ values have been estimated on the basis of the experimental data, if the k_1/k_2 ratio can be estimated, the individual k_1 and k_2 values can then be calculated from the combination of the k_1/k_2 ratio and overall rate constant ($k_1 + k_2$) values. We then used the method of initial rates, which is widely used in kinetic analyses,[31–33] because it does not rely on any assumptions about the reaction pathway, or the reversibility of reactions. We applied this method using the initial selectivity of primary products, i.e., the selectivity of products at close to zero conversion.[34] The k_1/k_2 ratio may be obtained directly from the initial selectivity ratio between primary products in the HYD and DDS pathways. The rate constant k_1 is proportional to the initial hydrogenation rate of 4,6-DMDBT to HDMDBTs, and the rate constant k_2 is proportional to the initial DDS rate of 4,6-DMDBT to DMBP. Figure 3 shows the plot of conversion versus selectivity for the 4,6-DMDBT HDS at 573 K and a H_2 pressure of 20.4 atm. HDMDBT and DMBP clearly are the primary products, and MCHT and DMBCH are the secondary products in 4,6-DMDBT HDS, because the selectivity for HDMDBT and DMBP at the zero conversion is nonzero and the selectivity for MCHT and DMBCH at the zero conversion is zero. The initial selectivity values for the primary products, HDMDBT and DMBP, can be determined by extrapolation to zero conversion and are 73.0% and 23.0%, respectively, for NiMo sulfide. The sum is 96%, which is similar to the expected value of 100%. The corresponding values are 47.5% and 41.3% for CoMo sulfide, respectively, which sum to 88.8%. The small deviation may be due to experimental error,

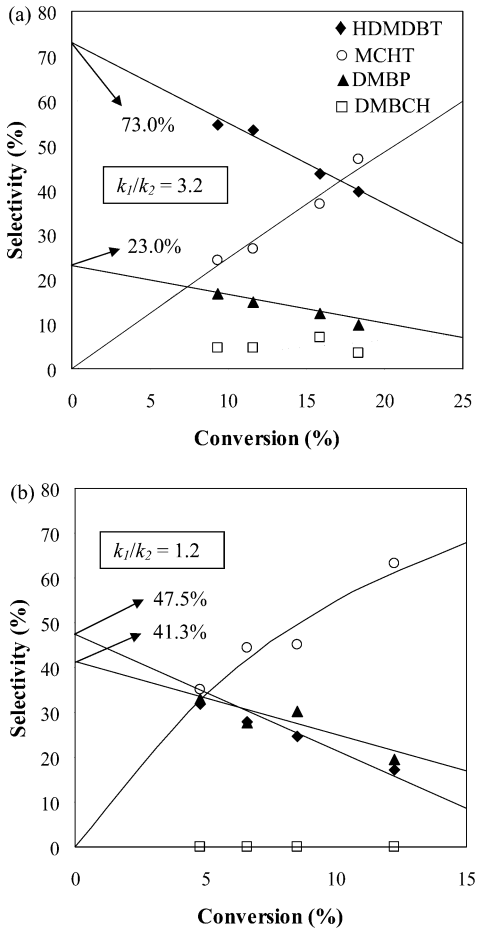

Figure 3. Extrapolation of hydrodimethyldibenzothiophene (HDMDBT) and 3,3′-dimethylbiphenyl (DMBP) products for estimating the initial selectivity of products over (a) NiMo sulfide and (b) CoMo sulfide. Temperature = 573 K, H_2 pressure = 20.4 atm.

because the data in this case are more scattered. The k_1/k_2 ratio is calculated from eq 2:

$$\frac{k_1}{k_2} = \frac{[\text{initial selectivity of HDMDBTs}]}{[\text{initial selectivity of DMBP}]} \qquad (2)$$

The ratio of k_1/k_2 is equal to 3.2 over NiMo sulfide and 1.2 over CoMo sulfide, as shown in Figure 3. Table 4 shows the individual rate constants for each reaction pathway calculated using this method. The rate constant for the HYD pathway over NiMo sulfide is 63.3 $\times$ 10^{-5} s^{-1} g·cat^{-1} at 573 K and a H_2 pressure of 20.4 atm, and this value is much higher than that for the DDS pathway, which is 19.9 $\times$ 10^{-5} s^{-1} g·cat^{-1}. Also, the rate constant for the HYD pathway over the NiMo sulfide is higher than that of CoMo sulfide, whose value is only 18.8 $\times$ 10^{-5} s^{-1} g·cat^{-1}.

3.4. Activation Energy of 4,6-Dimethyldibenzothiophene Hydrodesulfurization. Figure 4 shows Arrhenius plots for the NiMo and CoMo sulfide catalysts. The linearity (R) of data fitting was >0.97 for both catalysts. Table 5 summarizes the activation energies for the overall 4,6-DMDBT HDS and each reaction pathway, based on the individual rate constants for each reaction pathway. The activation energy of the overall 4,6-DMDBT HDS over NiMo sulfide was 12.6 kcal/mol, which is significantly lower than that over CoMo sulfide

(31) Lund, K.; Fogler, H. S.; McCune, C. C. *Chem. Eng. Sci.* **1973**, *28*, 691.
(32) Schwert, G. W. *J. Biol. Chem.* **1969**, *244*, 1278.
(33) Ernst, W. R. *Int. J. Chem. Kinet.* **1989**, *21*, 1153.
(34) Ma, X.; Peng, Y.; Schobert, H. H. *Prepr.—Am. Chem. Soc., Div. Pet. Chem.* **2000**, *45*, 488.

Table 4. Individual Rate Constants for HDS of 4,6-DMDBT and DBT

	20.4 atm, 548 K	20.4 atm, 573 K	20.4 atm, 598 K	13.6 atm, 573 K	40.8 atm, 573 K
		4,6-DMDBT			
NiMo sulfide catalyst					
$k_1 + k_2$ ($\times 10^{-5}$ s^{-1} g·cat^{-1})	60.0	83.2	159.3	55.2	133.5
k_1/k_2[a]	4.3	3.2	2.7	4.2	5.1
k_1 ($\times 10^{-5}$ s^{-1} g·cat^{-1})	48.6	63.3	115.8	44.6	111.6
k_2 ($\times 10^{-5}$ s^{-1} g·cat^{-1})	11.4	19.9	43.5	10.6	21.9
CoMo sulfide catalyst					
$k_1 + k_2$ ($\times 10^{-5}$ s^{-1} g·cat^{-1})	13.5	34.1	66.5		43.8
k_1/k_2[a]	2.3	1.2	1.2		2.7
k_1 ($\times 10^{-5}$ s^{-1} g·cat^{-1})	9.4	18.8	35.8		31.9
k_2 ($\times 10^{-5}$ s^{-1} g·cat^{-1})	4.1	15.3	30.7		11.9
		DBT			
NiMo sulfide catalyst					
$k_1 + k_2$ ($\times 10^{-5}$ s^{-1} g·cat^{-1})		212.3			
k_1/k_2[a]		0.1			
k_1 ($\times 10^{-5}$ s^{-1} g·cat^{-1})		25.3			
k_2 ($\times 10^{-5}$ s^{-1} g·cat^{-1})		187.0			
CoMo sulfide catalyst					
$k_1 + k_2$ ($\times 10^{-5}$ s^{-1} g·cat^{-1})		209.6			
k_1/k_2[a]		0.1			
k_1 ($\times 10^{-5}$ s^{-1} g·cat^{-1})		17.8			
k_2 ($\times 10^{-5}$ s^{-1} g·cat^{-1})		191.8			

[a] The k_1/k_2 ratio is determined by the initial product selectivity ratio ([initial selectivity of HDMDBTs]/[initial selectivity of DMBP]).

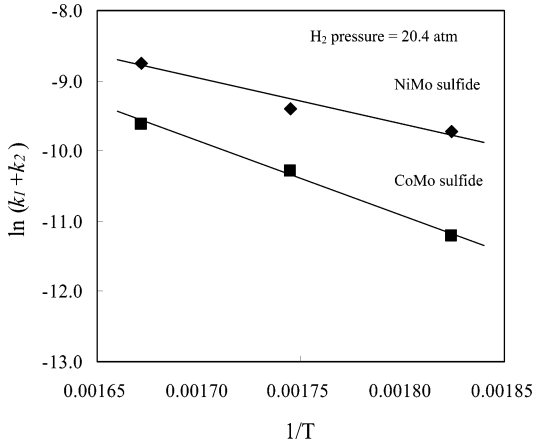

Figure 4. Arrhenius plot of the overall rate constants ($k_1 + k_2$) over NiMo sulfide and CoMo sulfide catalysts.

Table 5. Activation Energy for Individual Pathways of 4,6-DMDBT HDS

	Activation Energy (kcal/mol)
NiMo sulfide catalyst	
$E_{k_1+k_2}$	12.6
E_{k_1}	11.2
E_{k_2}	17.4
CoMo sulfide catalyst	
$E_{k_1+k_2}$	20.8
E_{k_1}	17.5
E_{k_2}	26.2

(20.8 kcal/mol). The activation energy for the HYD pathway (E_{k_1}) was less than that for the DDS pathway (E_{k_2}), indicating that the DDS pathway is more sensitive to reaction temperature.

3.5. Nickel Phosphide Catalysts for Deep Hydrodesulfurization. Nickel phosphide is an interesting type of new catalyst with good activity for deep HDS. Ni_2P/USY and Ni_2P/SiO_2 with a 5.9 wt % nickel metal loading were examined in this work. As shown in Table 1, this metal loading is less than the total metal loading in the NiMo and CoMo sulfide catalysts.

Table 6 compares the overall HDS rate constants and individual rate constants for each reaction pathway of 4,6-DMDBT HDS over the nickel phosphide catalysts, as well as over the sulfided NiMo and CoMo catalysts at 573 K and a H_2 pressure of 20.4 atm. Individual rate constants were calculated using the same method that was stated previously.

The overall HDS rate constants over the Ni_2P/USY and Ni_2P/SiO_2 were 51.5 $\times$ 10^{-5} and 66.4 $\times$ 10^{-5} s^{-1} g·cat^{-1}, respectively, in the HDS of 4,6-DMDBT, which were higher than that over CoMo sulfide, but lower than that over NiMo sulfide. Ni_2P/SiO_2 gave a very high k_1/k_2 ratio, with a value of 10.1, which is much higher than those over CoMo sulfide (1.23) and NiMo sulfide (3.19).

On the basis of the catalyst weight charged in the reactor, the rate constant for the HYD pathway over Ni_2P/USY and Ni_2P/SiO_2 were 43.2 $\times$ 10^{-5} and 60.4 $\times$ 10^{-5} s^{-1} g·cat^{-1}, respectively, which are much higher than that over CoMo sulfide (18.8 $\times$ 10^{-5} s^{-1} g·cat^{-1}) but lower than that over NiMo sulfide (63.3 $\times$ 10^{-5} s^{-1} g·cat^{-1}). However, the rate constants for the DDS pathway over the Ni_2P/USY and Ni_2P/SiO_2 were 8.3 $\times$ 10^{-5} and 6.0 $\times$ 10^{-5} s^{-1} g·cat^{-1}, respectively, which are less than those over the CoMo and NiMo sulfide catalysts.

4. Discussion

4.1. Hydrodesulfurization of 4,6-Dimethyldibenzothiophene. The reaction network for 4,6-DMDBT HDS is similar to that for DBT HDS, in that it has two major pathways (see Figure 1). In our study, DMBP was the only product from the DDS pathway, and, in the HYD pathway, the main products were 4HDMDBT and 6HDMDBT. MCHT and DMBCH, which are products of further hydrogenation, were also detected, whereas 12HDMDBT was not observed. Therefore, the hydrogenation reaction of 6HDMDBT to 12HDMDBT is likely to be very slow and, hence, negligible. For the reaction pathway of DMBP to MCHT during HDS of 4,6-DMDBT, this reaction has been reported to be very slow.[18] Generally, the reaction rate of BP to CHB is also very slow during DBT HDS. However, the hydrogena-

Table 6. Comparison of Weight-Based and Active-Site-Based Rate Constants over NiMo, CoMo Sulfides, and Nickel Phosphide Catalysts (Temperature = 573 K, H_2 Pressure = 20.4 atm)

	CoMo Sulfide	NiMo Sulfide	Ni_2P/USY	Ni_2P/SiO_2
$k_1 + k_2$ ($\times 10^{-5}$ s^{-1} g·cat^{-1})[a]	34.1 (4.0)[a]	83.2 (8.8)[a]	51.5 (15.2)[a]	66.4 (23.7)[a]
k_1/k_2	1.2	3.2	5.2	10.1
k_1 ($\times 10^{-5}$ s^{-1} g·cat^{-1})[a]	18.8 (2.2)	63.3 (6.7)	43.2 (12.7)	60.4 (21.6)
k_2 ($\times 10^{-5}$ s^{-1} g·cat^{-1})[a]	15.3 (1.8)	19.9 (2.1)	8.3 (2.5)	6.0 (2.1)

[a] The data in parentheses indicate active-site-based rate constant (given in units of s^{-1} active $site^{-1}$).

tion of DMBP to form MCHT is not negligible, because the selectivity for the formation of DMBP decreased by a factor of 3.3 at 25% conversion over NiMo and by a factor of 2.4 at 15% conversion over CoMo. Therefore, MCHT may be produced from both HYD and DDS reaction pathways. In this work, isomerization of 4,6-DMDBT is not considered, because this reaction is not significant for the types of catalysts studied under the conditions used, although isomerization is possible over acidic catalysts due to the migration of methyl groups at higher temperatures.

In the HDS of DBT, the DDS product (BP) is the main product and the hydrogenated products (CHB and BCH) are minor products, as shown in Table 2. Thus, in this reaction, the DDS pathway is dominant, in agreement with the results of other researchers.[35,36] In 4,6-DMDBT HDS, however, the HYD pathway is more dominant than the DDS pathway, as indicated by the individual rate constant for each reaction pathway. The rate constant for the HYD pathway, k_1, is larger than that for the DDS pathway, k_2, over the NiMo and CoMo sulfide catalysts under all reaction conditions, as shown in Table 4. However, in DBT HDS, the DDS pathways have a much larger rate constant than the HYD pathway. As shown in Table 5, the activation energy for the HYD pathway is less than that for the DDS pathway in 4,6-DMDBT HDS.

The reason 4,6-DMDBT produces more hydrogenated products than DBT is probably related to the blocking of the DDS pathway. Ma and co-workers[37,38] and Shafi and Hutchings[39] reported that the adsorption of 4,6-DMDBT on the active sites is hindered because of the two methyl groups on the 4- and 6-positions. If DMDBT is hydrogenated to hexahydro-DMDBT, this steric hindrance is reduced and the electron density on the S atom is increased, and, thus, the hydrogenated 4,6-DMDBT becomes easier to desulfurize.

On the other hand, Kabe and co-workers suggested that the methyl groups might inhibit the C−S bond scission of the adsorbed DBTs on the active sites.[40,41] They estimated the heats of adsorption for DBT, 4-MDBT, and 4,6-DMDBT by measuring the parameters in a simplified Langmuir−Hinshelwood equation. They reported that 4-MDBT and 4,6-DMDBT are adsorbed on the catalyst more strongly than DBT. Despite this phenomenon, the C−S scission of the substituted DBTs is retarded by the steric hindrance of the methyl groups.

Conflicting results were obtained in a recent study on the adsorption of DBT, 4-MDBT, and 4,6-DMDBT from the liquid phase onto NiMo and CoMo sulfide catalysts;[37] the adsorbed amount of DBT was observed to be larger than that of 4-MDBT and 4,6-DMDBT. This implies that the methyl groups at the 4- and 6-positions inhibit the interaction between the S atom in DBTs and the active sites (sulfur vacancies) on the catalyst (sulfur−metal species interaction). Furthermore, it was observed that the outlet concentrations of 4,6-DMDBT and 4-MDBT after the saturation point were higher than those in the feed. This means that DBT helped elute the 4-MDBT and 4,6-DMDBT from some adsorption sites, because of its higher adsorption strength than those of 4-MDBT and 4,6-DMDBT. In other words, DBT displaced some adsorbed 4,6-DMDBT on the surface. This experimental evidence points to the decreased adsorption of 4,6-DMDBT due to steric hindrance of the methyl groups.[37] A comparison with DBT HDS at 573 K under a H_2 pressure of 20.4 atm shows that the presence of the methyl groups at the 4- and 6-positions dramatically inhibited the DDS rate, because of steric hindrance around the S atom, but did not retard the HYD rate, thus making the HYD pathway more important, as can be seen from the k_2 and k_1 values for DBT versus 4,6-DMDBT over CoMo sulfide (for k_2 191.8 vs 15.3; for k_1: 17.8 vs 18.8) and NiMo sulfide (for k_2: 187.0 vs 19.9; for k_1: 25.3 vs 63.3). One conclusion that may be reached is that the methyl groups inhibit the adsorption of 4,6-DMDBT on the active sites for hydrogenolysis.

The steric hindrance in 4,6-DMDBT on adsorption can be visualized when its conformation and electron density are compared with that of DBT. Figure 5 displays the conformation of 4,6-DMDBT, DBT, and their hydrogenated products. The hydrogenated molecules are more distorted, giving better access of sulfur to the surface. Figure 6 displays the electron densities of DBT and 4,6-DMDBT. The figures show that, in DBT, which does not have any methyl groups, the S atom is accessible for bonding. It is likely that DBT can adsorb on an active site through a sulfur−metal interaction and can be desulfurized directly to BP.[23,42,43] The interaction through the π-electrons on the aromatic rings is less important and the hydrogenation to hexahydro-DBT, followed by desulfurization to CHB, is not favored.

In contrast, in the case of 4,6-DMDBT, the two methyl groups at the 4- and 6-positions inhibit the interaction

(35) Song, C. S.; Reddy, K. M. *Appl. Catal., A: Gen.* **1999**, *176*, 1.
(36) Kwak, C.; Kim, M. Y.; Choi, K.; Moon, S. H. *Appl. Catal., A: Gen.* **1999**, *185*, 19.
(37) Ma, X.; Kim, J. H.; Song, C. *Prepr. Pap.—Am. Chem. Soc., Div. Fuel Chem.* **2003**, *48*, 135.
(38) Ma, X.; Schobert, H. H. *Prepr. Pap.—Am. Chem. Soc., Div. Fuel Chem*. **1997**, *42*, 657.
(39) Shafi, R.; Hutchings, G. J. *Catal. Today* **2000**, *59*, 423.
(40) Kabe, T.; Ishihara, A.; Zhang, Q. *Appl. Catal., A: Gen.* **1993**, *97*, L1.
(41) Zhang, Q.; Ishihara, A.; Kabe, T. *Sekiyu Gakkaishi* **1996**, *39*, 410.
(42) Kilanowski, D. R.; Teeuwen, H.; De Beer, V. H. J.; Gates, B. C.; Schuit, G. C. A.; Kwart, H. *J. Catal.* **1978**, *55*, 129.
(43) Froment, G. F.; Depauw, G. A.; Vanrysselberghe, V. *Ind. Eng. Chem. Res.* **1974**, *33*, 2975.

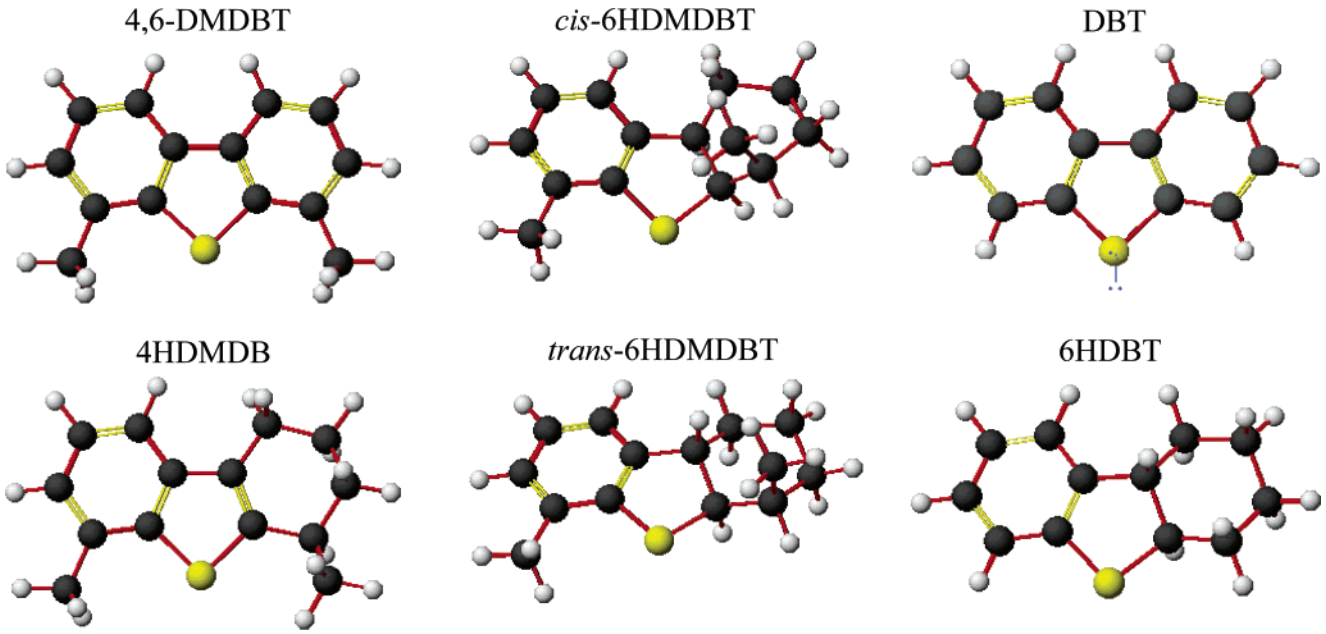

Figure 5. Conformation of 4,6-DMDBT, DBT, and their hydrogenated products.

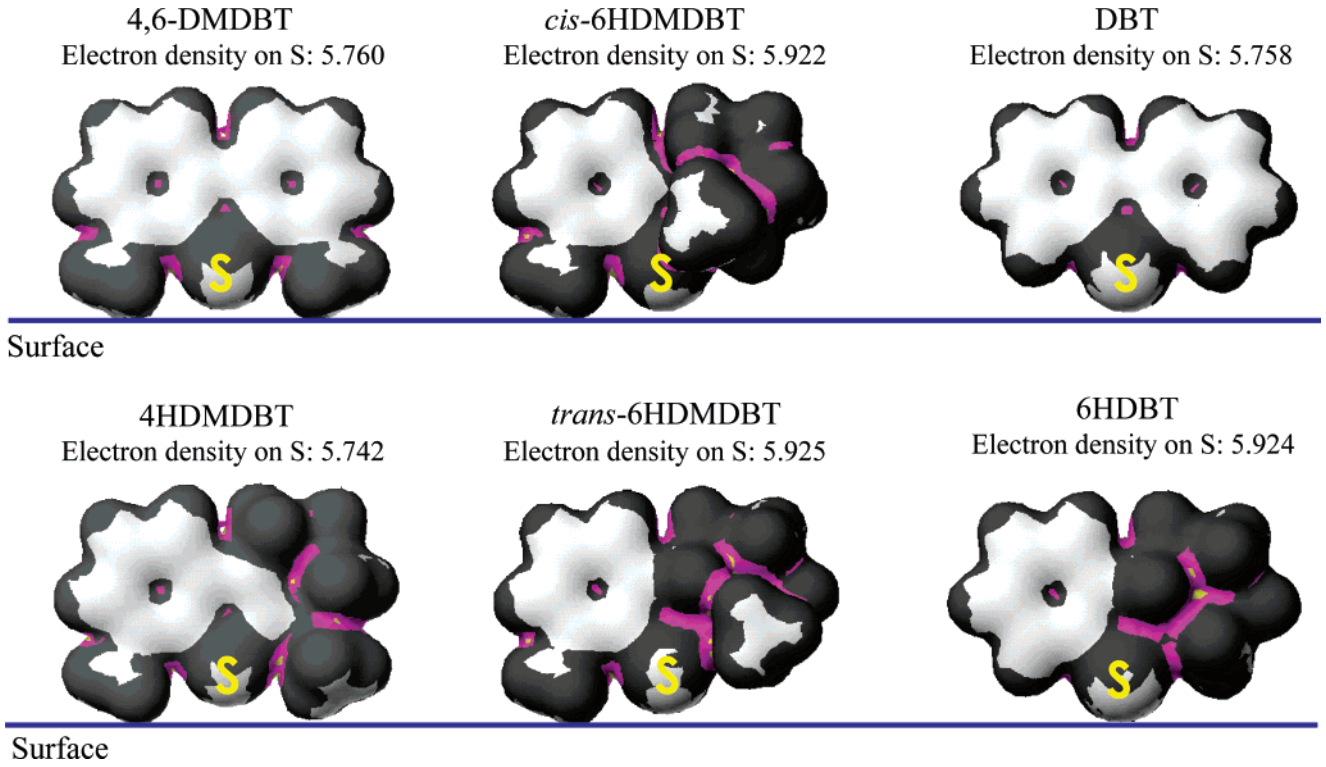

Figure 6. Electron density distribution of 4,6-DMDBT, DBT, and their hydrogenated products on isopotential surfaces.

of the S atom with the active site through a sulfur–metal bond. Therefore, 4,6-DMDBT prefers to adsorb on the active sites by forming a π-complex that can be hydrogenated to 4HDMDBT and 6HDMDBT. The hydrogenated products can then be desulfurized more easily, because of the changes in their electronic and steric properties. In particular, 6HDMDBT is much easier to desulfurize, because both its steric hindrance at the 4-position is greatly reduced, as shown in Figures 5 and 6, and the electronic density on the S atom increases significantly (from 5.76 for 4,6-DMDBT to 5.92 for 6HDMDBT). In conclusion, 4,6-DMDBT preferentially undergoes π-complexation rather than sulfur–metal interactions on the active site, leading to reaction by the HYD pathway rather than the DDS pathway. The NiMo sulfide is a more effective catalyst for 4,6-DMDBT HDS than the CoMo sulfide, because it has a better activity for the hydrogenation pathway.

It is well-known that CoMo and NiMo sulfide catalysts have good activity for HDS of thiophene-type sulfur compounds in liquid fuels,[44–47] with the CoMo sulfide

(44) Daage, M.; Chianelli, R. R. *J. Catal.* **1994**, *149*, 414.
(45) Girgis, M. J.; Gates, B. C. *Ind. Eng. Chem. Res.* **1991**, *30*, 2021.
(46) Kabe, T.; Ishihara, A. *Ind. Eng. Chem. Res.* **1992**, *31*, 1577.
(47) Quartararo, J.; Mignard, S.; Kasztelan, S. *J. Catal.* **2000**, *192*, 307.

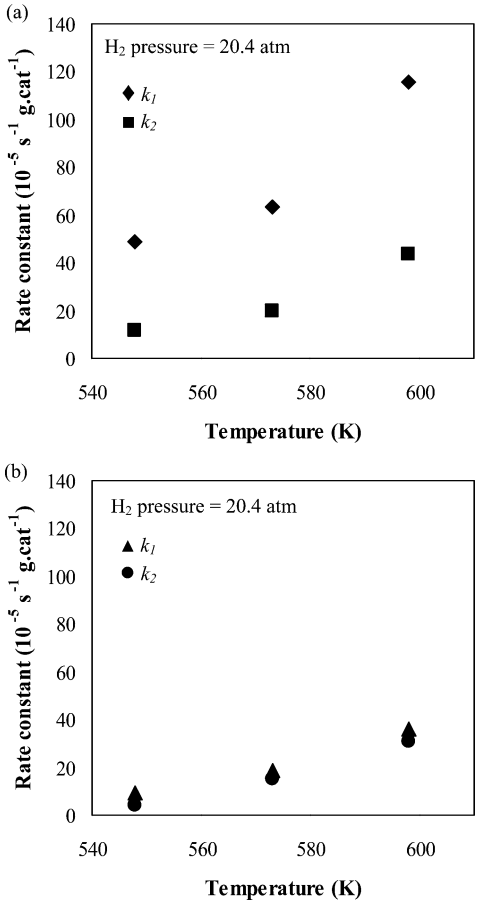

Figure 7. Effect of reaction temperature on HDS reaction pathway over (a) NiMo sulfide and (b) CoMo sulfide catalysts.

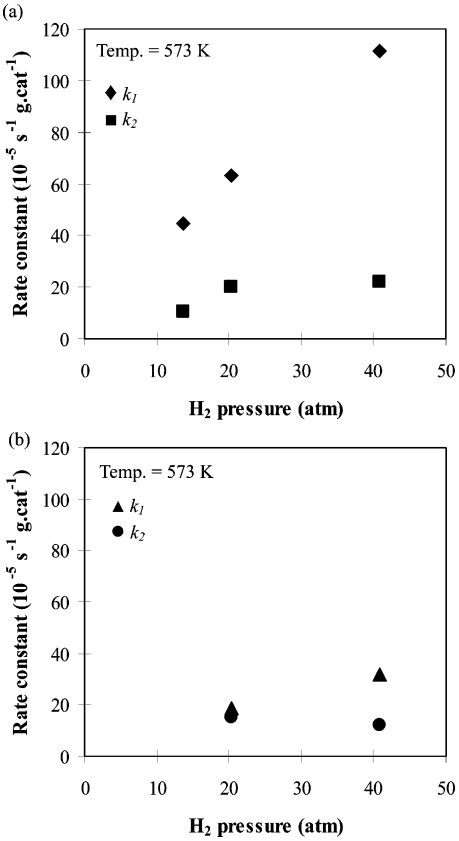

Figure 8. Effect of H_2 pressure on HDS reaction pathway over (a) NiMo sulfide and (b) CoMo sulfide catalysts.

catalyst favoring the DDS pathway and the NiMo catalyst favoring the HYD pathway. In the present study of the DBT HDS, it was duly noted that the CoMo sulfide catalyst produced primarily the desulfurized product, BP. Although this was also the main product on the NiMo sulfide catalyst, it also produced more hydrogenated products (CHB and BCH), as compared to the CoMo sulfide. The sum of the selectivities to hydrogenated products was 14.2% over CoMo sulfide and 35.6% over NiMo sulfide. This can be attributed to the higher hydrogenation activity of the NiMo sulfide than the CoMo sulfide, which is consistent with the known hydrogenation properties of nickel.

As shown in Figure 7, the rate constants for the two reaction pathways increase as the reaction temperature increases in the HDS of 4,6-DMDBT. For the NiMo catalyst, the rate constant for the DDS pathway (k_2) increased by a factor of 3.8, whereas the rate constant for the HYD pathway (k_1) increased by a factor of 2.4. This means that higher temperature favors the DDS pathway. H_2 pressure increased the rate constant for HYD pathway; however, the effect of H_2 pressure on the rate constant for DDS pathway is minor in the pressure range in this study, as shown in Figure 8. Consequently, the k_1/k_2 ratio was larger under high H_2 pressure, and, thus, increasing H_2 pressure favors the hydrogenation pathway.

Figures 7 and 8 show that the increase in rate constant with H_2 pressure (by 4-fold) is larger than that with reaction temperature (by 50 K). This does not necessarily mean that it is better to perform 4,6-DMDBT HDS at high H_2 pressure, because, in practice, the cost of the process changes must be taken into consideration.

4.2. Comparison of Rate Constants. Tables 7 and 8 compare the overall rate constants and activation energy values, respectively, for alkyldibezothiophene HDS over alumina-supported sulfide catalysts that have been reported by different research groups.[10,21,23,40,46,48,49] Because most researchers reported only the overall rate constant and activation energy of alkyl-DBTs HDS and performed the reaction at different reaction conditions, it is not easy to compare our kinetic data with the literature data. However, the overall rate constant from this work for NiMo sulfide (83.2×10^{-5} s^{-1} g·cat^{-1} at 573 K and 20.4 atm) is very similar to the rate constant (82.6×10^{-5} s^{-1} g·cat^{-1}) over NiMo sulfide that was reported by Sakanishi et al.,[21] although the H_2 pressure was higher in their reaction system. The trends in the kinetic data with increasing temperature are also similar. In the case of CoMo sulfide, however, our rate constant is less than that of Farag et al.,[23] and their rate constant increased more rapidly with increasing temperature. The two papers from the group of Mochida[21,23] did not report the activation energies over their catalysts. Because they performed HDS of 4,6-DMDBT and DBT at three different temperatures (573, 613 and 653 K), we calculated the activation energies with the Arrhenius law using their experimental data. The results are also shown in Table 8 for comparison.

(48) Kabe, T.; Akamatsu, K.; Ishihara, A.; Otsuki, S.; Godo, M.; Zhang, Q.; Qian, W. *Ind. Eng. Chem. Res.* **1997**, *36*, 5146.
(49) Kabe, T.; Akamatsu, K.; Ishihara, A.; Otsuki, S.; Godo, M.; Zhang, Q.; Qian, W.; Yamada, S. *Sekiyu Gakkaishi* **1999**, *42*, 150.

Table 7. Comparison of Overall Rate Constants for HDS of Alkyldibenzothiophenes over Alumina-Supported NiMo and CoMo Sulfide Catalysts Obtained from Independent Studies

Rate Constant (10^{-5} s^{-1} g·cat^{-1})				Reactor	Pressure			
DBT	4-MDBT	4,6-DMDBT	Temp (K)	Type	(atm)	Feed	Concentration	Reference
				$NiMo/Al_2O_3$ Catalyst				
		60.0	548	batch	20.4	Decalin	1.2 wt % 4,6-DMDBT	present work
212.2		83.2	573	batch	20.4	Decalin	1.2 wt % 4,6-DMDBT	present work
		159.3	598	batch	20.4	Decalin	1.2 wt % 4,6-DMDBT	present work
				$CoMo/Al_2O_3$ Catalyst				
		13.5	548	batch	20.4	Decalin	1.2 wt % 4,6-DMDBT	present work
209.6		34.1	573	batch	20.4	Decalin	1.2 wt % 4,6-DMDBT	present work
		66.5	598	batch	20.4	Decalin	1.2 wt % 4,6-DMDBT	present work
120.0		60.0	573	batch	28.6	Decane	1 wt % DBT and/or 0.1 wt % 4,6-DMDBT	Farag[23]
540.0		190.0	613	batch	28.6	Decane	1 wt % DBT and/or 0.1 wt % 4,6-DMDBT	Farag[23]
4350.0		800.0	653	batch	28.6	Decane	1 wt % DBT and/or 0.1 wt % 4,6-DMDBT	Farag[23]
				$NiMo/Al_2O_3$ Catalyst				
		82.6[a]	573	batch	29.6	Decane		Sakanishi[21]
		160.5[b]	613	batch	148.0	Decane		Sakanishi[21]
		277.0[c]	653	batch		Decane		Sakanishi[21]
				$CoMo/Al_2O_3$ Catalyst[d]				
116.7	33.3	24.7	593	flow	29.0	LGO	0.72 wt % sulfur	Kabe[48]
211.1	77.8	38.9	613	flow	29.0	LGO	0.72 wt % sulfur	Kabe[48]
333.3	125.0	41.7	623	flow	29.0	LGO	1.5 wt % sulfur	Kabe[48]
15.0	2.7	0.3	523	flow	39.5	LGO	1318 ppmw sulfur	Steiner[24]
48.0	11.0	3.3	548	flow	39.5	LGO	1318 ppmw sulfur	Steiner[24]
160.0	56.0	22.0	573	flow	39.5	LGO	1318 ppmw sulfur	Steiner[24]

[a] $k_1 = 68.8 \times 10^{-5}$ s^{-1} g·cat^{-1} and $k_2 = 13.8 \times 10^{-5}$ s^{-1} g·cat^{-1}. [b] $k_1 = 34.9 \times 10^{-5}$ s^{-1} g·cat^{-1} and $k_2 = 125.6 \times 10^{-5}$ s^{-1} g·cat^{-1}. [c] $k_1 = 17.1 \times 10^{-5}$ s^{-1} g·cat^{-1} and $k_2 = 259.9 \times 10^{-5}$ s^{-1} g·cat^{-1}. [d] The units for rate constant for the flow reactor data are 10^{-5} s^{-1}.

Table 8. Comparison of Apparent Activation Energies for HDS of Alkyldibenzothiophenes over Alumina-Supported NiMo and CoMo Sulfide Catalysts Obtained from Independent Studies

	Activation Energy (kcal/mol)							
Catalyst	DBT	4-MDBT	4,6-DMDBT	Reactor Type	Pressure (atm)	Solvent or Feed	Concentration	Reference
$NiMo/Al_2O_3$			12.6	batch	20.4	Decalin	1.2 wt % 4,6-DMDBT	present work
$CoMo/Al_2O_3$			20.8	batch	20.4	Decalin	1.2 wt % 4,6-DMDBT	present work
$NiMo/Al_2O_3$			11.3[a]	batch		Decane		Sakanishi[21]
$CoMo/Al_2O_3$	33.2[a]		24.0[a]	batch	28.6	Decane	0.1 wt % 4,6-DMDBT	Farag[23]
$NiMo/Al_2O_3$	28.7	36.1	53.0	flow	39.5	LGO	1318 ppmw sulfur	Steinner[24]
NiMo	24.0	31.0	40.0	flow		Decalin	0.1−0.4 wt % DBTs	Kabe[40]
CoMo	22.0	27.0	31.0	flow	29.0	LGO	0.168 wt % sulfur	Kabe[49]
CoMo	27.0	28.0	27.0	flow	29.0	LGO	1.5 wt % sulfur	Kabe[49]
$NiMo/Al_2O_3$	26.0		31.9	flow	48.4	Decalin	0.1−0.4 wt % DBTs	Kabe[10]
NiW/Al_2O_3	24.7		32.8	flow	48.4	Decalin	0.1−0.4 wt % DBTs	Kabe[10]
Mo/Al_2O_3	26.0		30.0	flow	48.4	Decalin	0.1−0.4 wt % DBTs	Kabe[10]
$CoMo/Al_2O_3$	25.0		31.0	flow	48.4	Decalin	0.1−0.4 wt % DBTs	Kabe[10]
$CoMo/Al_2O_3$	26.0	29.0	31.0	flow	29.0	LGO	1.5 wt % DBT	Kabe[48]
$CoMo/Al_2O_3$	27.0	28.0	27.0	flow	29.0	LGO	1.5 wt % DBT	Kabe[48]

[a] Calculated by the present authors, using the data of Sakanishi et al.[21] reported in Table 7.

The activation energy values from our calculation using their data for 4,6-DMDBT are 11.3 kcal/mol over NiMo sulfide and 24.0 kcal/mol over CoMo sulfide, and these values are very similar to the activation energies over NiMo (12.6 kcal/mol) and CoMo sulfide (20.8 kcal/mol) that have been obtained in our own work.

Sakanishi et al.[21] also reported individual rate constants for 4,6-DMDBT reactions, as shown in Table 7. The rate constants for the HYD pathway (k_1) and the DDS pathway (k_2) values over NiMo sulfide at 573 K are very similar to our kinetic data. However, in their report, k_1 over the NiMo sulfide decreased as the temperature increased, whereas k_2 increased dramatically. This trend is different from that in our work. In our results, k_1 still increases as the temperature increases, although HDS was performed at lower temperature, as compared with that used by Farag et al.[23]

In the reports by Mochida and co-workers,[21,23] the rate constants were calculated according to a computer curve-fitting of plots of yield versus time, and reaction data were collected from low conversion to a high conversion of ~90%. They fitted each product yield with a curve-fitting method; however, the procedure was not described in detail in their papers. In the present study, a simple method of analysis was used with data collected at low conversion (generally values of <20%) and the rates fit first-order kinetic expressions well.

Because we used the overall rate constant ($k_1 + k_2$) under low conversion and the initial selectivities to estimate the individual rate constants, the effect of the HDS products, such as H_2S, on the rate constants of initial reactions is negligible, and therefore, the k_1 and k_2 values estimated in this study do not include the effect of H_2S at high concentrations.

4.3. Nickel Phosphide Catalysts for Deep Hydrodesulfurization. Oyama et al.[11] and Stinner et al.[12] have recently reported that transition-metal phosphides are promising materials for next-generation catalysts.

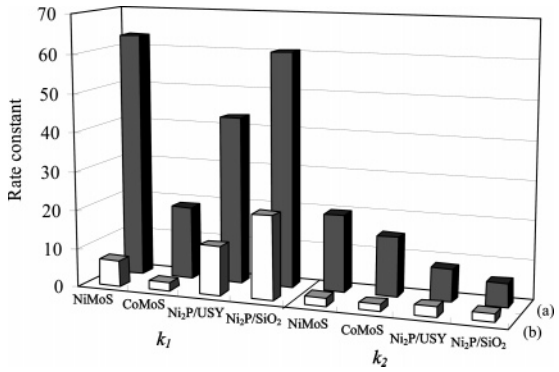

Figure 9. Comparison of (a) catalyst weight-based rate constants (in units of 10^{-5} s^{-1} g·cat^{-1}) and (b) active-site-based rate constants (in units of s^{-1} active site^{-1}) for individual HDS reaction pathways over NiMo sulfide, CoMo sulfide, and nickel phosphide catalysts. Temperature = 573 K, H_2 pressure = 20.4 atm.

Among the phosphides studied, nickel phosphide (Ni_2P) has the highest activity for HDS and hydrodenitrogenation (HDN), and it has higher activity for these reactions than sulfided commercial $NiMo/Al_2O_3$ catalysts, based on equal sites loaded in the reactor.[13]

In the present work, nickel phosphide catalysts showed greater activity than CoMo sulfide, but less than NiMo sulfide, on a weight basis, as shown in Table 6. It is very interesting that nickel phosphide catalysts have very high k_1/k_2 ratios, as compared with NiMo and CoMo sulfides. The k_1/k_2 ratios over Ni_2P/SiO_2 and Ni_2P/USY are 10.1 and 5.2, respectively, which are higher than those over NiMo sulfide (3.2) and CoMo sulfide (1.2). This means that nickel phosphide favors the HYD pathway more than the DDS pathway for 4,6-DMDBT HDS. These values were based on the total amount of catalyst loaded.

If the rate constants were calculated using the number of active sites, the results would favor the nickel phosphide, because it has lower metal loading and a lower number of active sites, as compared to NiMo and CoMo sulfide catalysts. In a catalyst evaluation study with an unoptimized catalyst, it is reasonable to compare the activity based on active sites to obtain a measure of the intrinsic rate. A high intrinsic rate would justify further research for improvement of the catalyst. In this study, chemisorption of CO and O_2 were used to estimate the number of active sites on the nickel phosphide and the sulfides, respectively. The CO method is reasonable for giving the number of surface metal atoms in phosphides.[11,50] The O_2 method, which is applied at dry ice/acetone temperatures in a pulse manner, is similarly reasonable for estimation of the sites on sulfides,[51,52] because corrosive chemisorption does not occur using this procedure.[53]

Table 6 and Figure 9 compare the rate constants on the basis of catalyst weight and active sites. The active-site-based overall HDS rate constants with Ni_2P/USY and Ni_2P/SiO_2 are 15.2 and 23.7 s^{-1} active site^{-1}, respectively, and these are much higher than those over NiMo and CoMo sulfide catalysts, which are 8.8 and 4.0 s^{-1} active site^{-1}, respectively.

For the HYD pathway, the rate constants over Ni_2P/USY and Ni_2P/SiO_2 are 12.7 and 21.6 s^{-1} active site^{-1}, respectively, and the corresponding values for the DDS pathway are 2.5 and 2.1 s^{-1} active site^{-1}, respectively. The rate constant for the HYD pathway over Ni_2P/SiO_2 is much larger than those over sulfide catalysts (a factor of 3.2 or 9.8, respectively, larger than those over the NiMo or CoMo sulfide catalysts). On the basis of active sites, the rate constants for the DDS pathway over nickel phosphides are similar to, or only slightly larger than, those over NiMo and CoMo sulfides. This means that the activity for the HYD pathway is much more important than the DDS pathway for the nickel phosphide catalyst in the HDS of 4,6-DMDBT.

In the previous section, it was mentioned that the HDS of 4,6-DMDBT proceeded more readily via the HYD pathway than via the DDS pathway. Therefore, a catalyst might have very good activity in the HDS of 4,6-DMDBT if it promotes ring hydrogenation. This was the case for nickel phosphide, which, on an active-site basis, showed better performance for the HDS of 4,6-DMDBT than the sulfided commercial catalysts.

In addition to the results presented in this work, we have performed some experiments at the high conversion levels, in regard to the differences at higher conversions, and the conclusions are valid concerning the tendencies of the relative performances between the sulfide and phosphide catalysts. The nickel phosphide remains superior to sulfided $NiMo/Al_2O_3$ and still operates via the HYD pathway. We have also examined the effect of sulfur concentration in the feed with a varying dimethyl disulfide (DMDS) content (0%, 0.3%, and 0.6% sulfur). At a low temperature (e.g., 573 K), the addition of a DMDS led to little change in HDS catalytic activity and the product selectivities were not affected. At a high temperature (613 K), the addition of a DMDS (up to 0.6% sulfur) led to a small decrease in the HDS conversion and a decrease in the HYD selectivity. The selectivity to DDS pathway was increased and approached that of a sulfided $NiMo/Al_2O_3$. These results indicate that the Ni_2P phase undergoes a partial sulfidation with high sulfur concentration feed at a high temperature (613 K), as also indicated by extended X-ray absorption fine structure (EXAFS) analysis results on the spent samples. Despite a high sulfur content of 0.65% at a high temperature of 613 K, the Ni_2P/SiO_2 catalyst (EH5) maintained high HDS and HDN activity, as revealed by the results from laboratory testing (not shown here).

The nickel phosphides used in this work had a nickel loading of 5.9 wt %, which was low compared with the total metal loading in the NiMo and CoMo sulfide catalysts (>15 wt %). Therefore, nickel phosphide is a promising new type of catalyst for deep HDS. It may be further improved by increasing the amount of nickel loading and dispersion on the support.

5. Conclusions

The kinetics for the hydrodesulfurization (HDS) of 4,6-dimethyldibenzothiophene (4,6-DMDBT) over two sulfide catalysts and two new nickel phosphide catalysts

(50) Clark, P. A.; Oyama, S. T. *J. Catal.* **2003**, *218*, 78.
(51) Tauster, S. J.; Pecoraro, T. A.; Chianelli, R. R. *J. Catal.* **1980**, *63*, 515.
(52) Zmierczak, W.; Muralidhar, G.; Massoth, F. E. *J. Catal.* **1982**, *77*, 432.
(53) Bodrero, T. A.; Bartholomew, C. H.; Pratt, K. C. *J. Catal.* **1982**, *78*, 253.

were evaluated. Both the overall and individual rate constants in the reaction network were determined. The individual rate constants for direct desulfurization (DDS, or hydrogenolysis) and hydrogenation (HYD) pathways were determined by a combination of the overall rate constant and the initial selectivities. This method did not require any assumptions about the individual steps in the reaction network and is considered to be a more reliable method.

The HDS of 4,6-DMDBT proceeded mainly through a HYD pathway on all the catalysts, whereas the HDS of DBT proceeded predominantly through a DDS pathway. The overall rate constants for 4,6-DMDBT HDS ($k_1 + k_2$) on a catalyst weight basis (in units of 10^{-5} s^{-1} $g{\cdot}cat^{-1}$) at 573 K under a pressure of 20.4 atm increased in the order of CoMo sulfide (34.1) < Ni_2P/USY (51.5) < Ni_2P/SiO_2 (66.4) < NiMo sulfide (83.2); however, the values based on active sites (s^{-1} active $site^{-1}$) ranked in a different order of CoMo sulfide (4.0) < NiMo sulfide (8.8) < Ni_2P/USY (15.2) < Ni_2P/SiO_2 (23.7). The rate constants for the HYD pathway of 4,6-DMDBT HDS based on active sites were strongly dependent on the type of catalyst used at 573 K; however, those for the DDS pathway were less sensitive to the type of catalyst, as can be observed from the corresponding values (k_1; k_2) for CoMo sulfide (2.2; 1.8), NiMo sulfide (6.7; 2.1), Ni_2P/USY (12.7; 2.5), and Ni_2P/SiO_2 (21.6; 2.1).

From a comparison between the HDS of 4,6-DMDBT and DBT at 573 K and a H_2 pressure of 20.4 atm, it was determined that the presence of the methyl groups at the 4- and 6-positions dramatically inhibited the DDS pathway and, thus, made the HYD pathway more important. This was indicated by the k_2 (for DDS) and k_1 (for HYD) values for DBT versus 4,6-DMDBT over CoMo sulfide (for k_2: 191.8 vs 15.3; for k_1: 17.8 vs 18.8) and NiMo sulfide (for k_2: 187.0 vs 19.9; for k_1: 25.3 vs 63.3).

Based on molecular simulations and liquid-phase adsorption experiments, the much lower k_2 value for 4,6-DMDBT (compared to the k_2 value for DBT) was due to steric hindrance by the methyl groups in 4,6-DMDBT, which inhibited its adsorption through the S atom and resulted in great suppression of the k_2 values. 4,6-DMDBT adsorbed on the catalyst surface preferentially via a π-complex, which led to ring hydrogenation and resulted in higher k_1 values in the catalysts that have high hydrogenation capability. NiMo sulfide showed better performance than CoMo sulfide, because it gave much higher k_1 values for the HYD pathway. In fact, the rate for HYD (k_1) with NiMo sulfide at 573 K under a pressure of 20.4 atm is higher for 4,6-DMDBT HDS (63.3) than that for DBT HDS (25.3), although the overall rate constant was much lower for the former (83.2) than for the latter (212.3), because of suppression of the DDS pathway for 4,6-DMDBT HDS.

For the DDS pathway of 4,6-DMDBT HDS, the activity of the nickel phosphides is not significantly different from that of NiMo or CoMo sulfide. However, the nickel phosphide catalyst showed much higher intrinsic activity for the HYD pathway than the sulfides on an active-site basis for 4,6-DMDBT, and its excellent performance can be attributed to its excellent hydrogenation ability. Therefore, nickel phosphide catalysts are a promising new type of catalyst for deep HDS, which requires refractory sulfur compounds to react more through the HYD pathway than the DDS pathway.

Acknowledgment. This work was supported in part by the New Energy and Industrial Technology Development Organization (NEDO) of Japan (through its international grant), the U.S. Department of Energy/National Energy Technology Laboratory (through UCR Grant No. DE-FG26-00NT40821), the U.S. Environmental Protection Agency (through TSE Grant No. R831471), and the Office of Basic Energy Sciences (through Grant No. DE-FG02-963414669), as well as the Postdoctoral Fellowship (to J. H. Kim) of the Korea Science and Engineering Foundation (KOSEF).

EF049804G